Usage Report for Fiscal Year 2018

Project Title:

The numerical analysis of oxygen transport in the microcapillary.

Name:

○ Xiaolong Wang

Laboratory at RIKEN:

Head Office for Information Systems and Cybersecurity

Computational Engineering Applications Unit

1. Background and purpose of the project, relationship of the project with other projects

Red blood cells continuously transport oxygen from the lungs to the capillaries near the tissue during their 120-day lifespan. The role of cell membranes, which are an important component of red blood cells, in this process is attracting more and more attention. Cell membranes, while protecting cell organelles from their surrounding micro-environment, also allow nutrient transfer and facilitate cellular communication via transmembrane ionic currents. They are necessarily permeable to the low-molecular-weight substance as oxygen, and semi-permeable to ionic species and water (through special channels or membrane-borne proteins like AQP1). Understanding mass transfer across permeable biomembranes is of great importance for studying cell mechanics and biological functions of living organisms.

It has long been noted that the magnitude and the direction of water flux across cell membranes is related to the difference of hydraulic and osmotic pressure as introduced by Katchalsy & Curran in 1965 [3]. Different from adherent cells spreading on substrates, red blood cells (RBCs) in motion often present large deformation when they go through a microcirculation system [4]. For the mass transfer through flexible and permeable membranes in motion, how the permeability of cell membranes, coupled with the fluid–membrane interaction, affects the mass transfer efficiency, is still an open question.

2. Specific usage status of the system and calculation method

In FY2018, about 700,000 core*hours were used for my Quick Use project. We used a parallel program based on OpenMp and MPI to numerically simulate cell movement and mass transfer.

In the present work, we considered an immersed porous interface $\mathbf{X}_m$ with thickness h and permeability coefficient K in incompressible fluids as shown in Fig. 1. The porosity per unit surface area is assumed and characterized as a one-dimensional porous channel for fluids and diffusive substances inside the membrane.

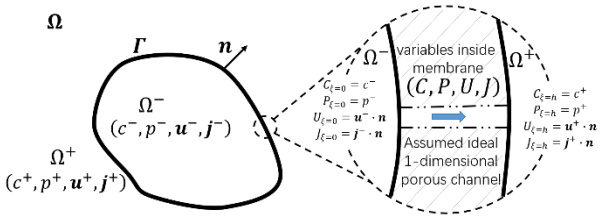

Figure 1. Sketch of the mass transfer through immersed porous interface with an ideal one-dimensional channel embedded in the membrane.

The concentration c of a substance satisfies the convection-diffusion equation,

$$c_t^{\pm} + \mathbf{u}^{\pm} \cdot \nabla c^{\pm} = \nabla \cdot (D \nabla c^{\pm}) \qquad (1)$$

in the sub-domain $\Omega^{\pm}$ separated by the moving interface marked as Γ. Take the spatial gradient on both sides, we have

$$\left(\boldsymbol{j}_D^{\pm}\right)_t + \nabla\left(\boldsymbol{u}^{\pm} \cdot \boldsymbol{j}_D^{\pm}\right) = D \nabla\nabla \cdot \boldsymbol{j}_D^{\pm} \qquad (2)$$

Here **u** is the velocity of the surrounding liquid, and D is the diffusion coefficient of the substance in liquid. Mass flux through permeable interface relative to interface, i.e., moving with the interface on either side is formulated as

$$\mathbf{j}_{\Gamma}^{\pm} = U c^{\pm} \mathbf{n} - D \nabla c^{\pm} \qquad (3)$$

where U is the transmembrane velocity through the

interface via a porous channel, and $\mathbf{n}$ stands for the unit normal vector of the membrane. The fluid velocity through the interface is formulated with Darcy's law in the normal direction as

$$U = -\frac{K}{\mu}\frac{dP}{d\xi} \tag{4}$$

By integrating along the thickness of the membrane, we obtain

$$U = -\frac{K}{\mu h}[p] \tag{5}$$

In this study, we extended the immersed boundary method in Gong el at.[1]. The cell membrane is considered to be a homogeneous isotropic porous medium. The solvent flux through the membrane depends on the pressure gradient across the membrane, the viscosity of the fluid and the membrane permeability. The solute flux contains contributions from both convection and diffusion. The specific derivation process is omitted, and the final governing equations based on immersed boundary framework are as follows.

$$\nabla \cdot \boldsymbol{u} = 0,$$

$$\rho\frac{\partial \boldsymbol{u}}{\partial t} + \rho(\boldsymbol{u}\cdot\nabla)\boldsymbol{u} = -\nabla p + \nabla\cdot\mu(\nabla\boldsymbol{u} + \nabla\boldsymbol{u}^T) + \boldsymbol{f},$$

$$\boldsymbol{f}(\boldsymbol{x},t) = \int_\Gamma \boldsymbol{F}(\boldsymbol{X},t)\delta(\boldsymbol{x}-\boldsymbol{X})\mathrm{d}\boldsymbol{X},$$

$$\boldsymbol{F} = -(\boldsymbol{P}\cdot\nabla)\cdot(\boldsymbol{\tau} + \boldsymbol{q}\boldsymbol{n}),$$

$$\boldsymbol{q} = \big((\boldsymbol{P}\cdot\nabla)\cdot\boldsymbol{m}\big)\cdot\boldsymbol{P} \text{ and } \boldsymbol{m} = E_b(\boldsymbol{P}\cdot\nabla\boldsymbol{n} - k_m^R\boldsymbol{P}),$$

$$\boldsymbol{\tau} = \frac{2}{\lambda_1\lambda_2}\frac{\partial W_s}{\partial I_1}\boldsymbol{B}^s + 2\lambda_1\lambda_2\frac{\partial W_s}{\partial I_2}\boldsymbol{P},$$

$$\frac{\mathrm{d}\boldsymbol{X}}{\mathrm{d}t} = -U\boldsymbol{n} + \int_\Omega \boldsymbol{u}(\boldsymbol{x},t)\delta(\boldsymbol{x}-\boldsymbol{X})\mathrm{d}\boldsymbol{x},$$

$$U = -\frac{K}{\mu h}\frac{\boldsymbol{F}\cdot\boldsymbol{n}}{|\boldsymbol{X}_s|}. \tag{6}$$

The mass transportation equation of solute concentration c and diffusion flux $\boldsymbol{j_D}$ in a monolithic form, i.e., immersed boundary method style formulation are as follows,

$$c_t + \boldsymbol{u}\cdot\nabla c = \nabla\cdot\Big\{D\nabla c + D\int_\Gamma \boldsymbol{n}\Theta(\boldsymbol{j}_\Gamma\cdot\boldsymbol{n} - Uc)\delta(\boldsymbol{x}-\boldsymbol{X})\mathrm{d}\boldsymbol{X}\Big\}$$
$$= \nabla\cdot\{D\nabla c + D\textstyle\int_\Gamma \boldsymbol{n}\Theta(\boldsymbol{j}_D\cdot\boldsymbol{n})\delta(\boldsymbol{x}-\boldsymbol{X})\mathrm{d}\boldsymbol{X}\} \tag{7}$$

$$(\boldsymbol{j_D})_t + (\boldsymbol{u}\cdot\boldsymbol{\nabla}\boldsymbol{j_D}) + (\boldsymbol{\nabla}\boldsymbol{u})\cdot\boldsymbol{j_D} = \boldsymbol{D}\boldsymbol{\nabla}\{\boldsymbol{\nabla}\cdot\boldsymbol{j_D} - \textstyle\int_\Gamma(\Psi\boldsymbol{j_D}\cdot\boldsymbol{n})\boldsymbol{\delta}(\boldsymbol{x}-\boldsymbol{X})\boldsymbol{dX}\} \tag{8}$$

in which $\Theta = \frac{2}{|U|}\tanh\left(\frac{Pe_m}{2}\right), \Theta = 2\tanh\left(\frac{Pe_m}{2}\right)$, $Pe_m = \frac{|U|h}{D_m}$. The combination of Eqs. (7) and (8) provides a complete set of the governing equations for mass transfer through a porous interface.

The whole blood flow in microvessels will be studied numerically with 3D simulations. The immersed boundary method is used to model the interaction between fluid and blood cells. The membrane of the blood cell is treated as a hyper-elastic thin shell. The continuity equation and momentum equation will be solved using the SMAC method. To ensure stability when updating the membrane position, we used the second-order Runge-Kutta method.

3. Result

To validate the proposed method, mass transfer through a shrinking porous circular membrane in a two-dimensional setting is predicted and compared with its semi-analytical solution. For simplicity, we considered a circular linear elastic membrane without bending rigidity. The membrane expands uniformly to twice its reference radius as $2r_0$, and set this stressed configuration as its initial state. The membrane will shrink back to its reference configuration under the in-plane elastic stress. For the present setup with circular symmetry, zero flow velocity naturally satisfied the Navier-Stokes equation for this specific shrinking problem as a unique solution. Figure 2 shows that our numerical results are consistent with the theoretical solution.

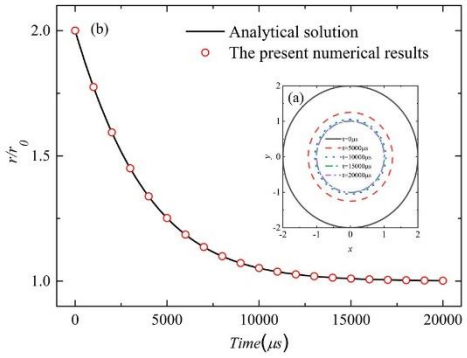

Figure 2. Validation of the proposed method with shrinking of a circular porous membrane from its initial radius $2r_0$ to its reference configuration r_0 : (a) shapes of the membrane at various times during the shrinking process; (b) comparison of the radius variation between numerical and analytical results.

As an application of the proposed method, the effect of membrane permeability on oxygen unloading from RBCs in a circular pipe with 10 μm in diameter and 12 μm in length is investigated. Parameter values adopted in the present numerical study are shown in Table 1. The Skalak hyperelastic membrane model and the Pozrikidis bending stress model were used for predicting membrane stress as described in Gong et al. [1]. The circular channel is defined with VOF functions in a 12×12×12 μm^3 cube . No-slip conditions were used on the pipe boundary. Periodic conditions were used in the axial (flow) direction for velocity and concentration with the flow driven by a pressure drop along the flow inside the channel.

The spatial variation of transmembrane velocity, are illustrated in Fig. 3. As shown in the figure, the diffusive flux through the membrane is the main factor for oxygen unloading, and the transmembrane flux is about two orders of magnitude smaller compared to the diffusive flux. The transmembrane velocity is positive when fluid flows out of the cell in the front, and takes negative values as the flow reverses in the rear, which is consistent with the stress-state of the cell membrane. The membrane in the front region is being stretched, while the rear region is being compressed inside the micro channel flow.

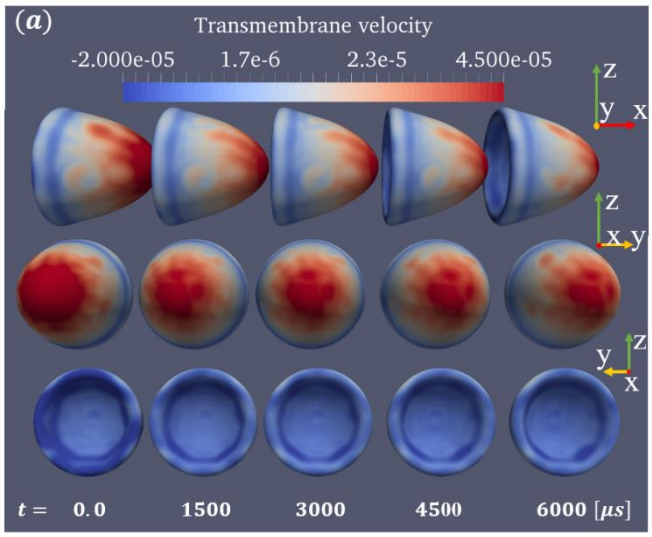

Figure 3. Contours of the magnitude of transmembrane velocity distributions on a moving and deformed cell membrane.

Fig. 4 shows the effects of membrane permeability on the local flow field next to the deformed cell membranes. As shown in Fig. 4a, fluid flow inside the domain encapsulated by a porous membrane is enhanced compared to that of a nonporous membrane. The vorticity inside the encapsulated region near the front of the membrane, and outside the membrane close to the rear of the membrane, is much greater for a permeable membrane than a nonporous membrane as shown in Fig. 4b. The vorticity on both sides of the membrane is calculated and interpolated onto the cell membrane as shown in Fig. 4c. The results indicate that its value near the membrane increases nonlinearly with the membrane permeability coefficients.

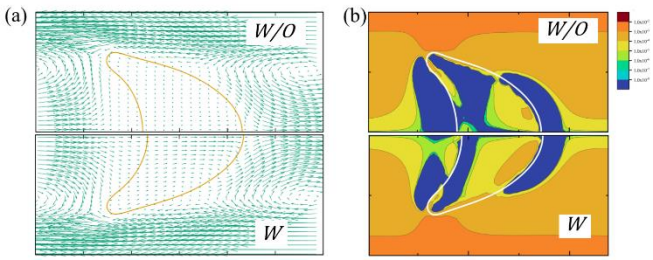

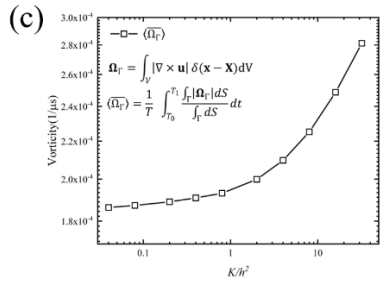

Figure 4. Effect of membrane permeability on the local hydrodynamics around the deformed cell membranes. (a) Relative velocity of the flow field to the centroid velocity of the cell, $\mathbf{u}-\mathbf{U}_c$, with/without membrane permeability, (b) the contours of the vorticity in flow field, $|\nabla \times \mathbf{u}|$, with/without membrane permeability, (c) the averaged of the vorticity near cell membrane.

4. Conclusion

An immersed boundary method for modeling convection and diffusion mass through a deformable membrane with porosity was proposed in this paper. The membrane was modeled based on Darcy's law as porous media. The concentration jump over the interface was described with a hyperbolic function in which a membrane Pelect number was introduced. A diffusive flux equation was derived and coupled with the concentration equation for a stable solution of the mass transfer in the immersed boundary style. The present numerical method presents a robust capacity for solving the concentration field with an oscillation membrane.

As an application, oxygen unloading from the RBCs with large deformations in a micro channel was investigated. Numerical results suggest that for low Peclet number mass transfer with porous bio-membrane in micro channels, membrane permeability changes local hydrodynamic conditions, such as vorticity, close to the membrane, which facilitates the diffusion around the membrane and enhances the mass transfer efficiency.

5. Schedule and prospect for the future

We have completed numerical analysis of mass transfer in a 10 μm microvessel, and we have found that solvents and solutes exhibit different patterns on cell membrane. As is shown in Fig. 5. Along the profile of the deformed RBC, three distict regions of the transmembrane velocity can be obersved. The velocity decreases from the outflow region in the front to a transient region around the tip, and an inflow region in the rear.

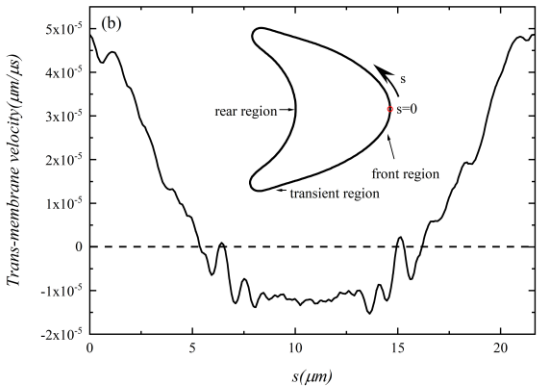

Figure 5. Transmembrane velocities along the cell membrane of a deformed red blood cell.

Next, we would like to explore the corresponding changes of the ratio of area of the inflow region and that of outflow regions on the cell membrane in the capillaries with different diameters, especially in the capillaries with a diameter smaller than erythrocyte.

Fedosov[2] employed mesoscale hydrodynamic simulations to predict the phase diagram of shapes and dynamics of RBCs in cylindrical microchannels, and found that a rich dynamical behavior (i.e. snaking and tumbling discocytes, slippers performing a swinging motion, and stationary parachutes) with different shear rates in capillaries with different diameters. The stable shape of RBC at different shear rates is shown in Figure 6. Recent studies of the effects of different steady state of RBC on the oxygen release in capillaries provide new insights into the questions: (1) Does the transport of the solvent across the cell membrane affect the final state of the cell? (2) will the changes of steady shape of RBC at different shear rates tube promote oxygen transport more efficiently to the tissue? Next we will do a series of

numerical experiments to explore these two issues.

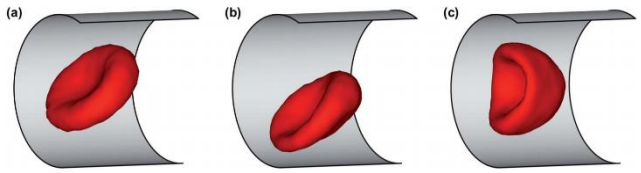

Figure 6. Simulation snapshots of a RBC in flow as dimensionless flow rate $\dot{\gamma}^* = (a)5{,}24.\,(b)8,(c)59.6$[2]

Currently, I have a “Quick Use” user account and I would like to get extension of computation facilities for next usage term (up to 31st March 2020) under the same user category.

References:

[1] Xiaobo Gong, Zhaoxin Gong, Huaxiong Huang; “An immersed boundary method for mass transfer across permeable moving interfaces”; Journal of Computational Physics, Volume 278, 1 December 2014, Pages 148–168.

[2] Dmitry A. Fedosov, Matti Peltomäkia ,Gerhard Gompper; “Deformation and dynamics of red blood cells in flow through cylindrical microchannels”; Soft Matter, 2014, 10, 4258.

[3] Katchalsky K. & Curran P.F., Non-equilibrium Thermodynamics in Biophysics. Cambridge, MA: Harvard University Press, 1965.

[4] Secomb, T.W., Blood flow in the microcirculation, Annual Review of Fluid Mechanics, 49:443-461, 201